Journal of Thermal Analysis and Calorimetry, Vol. 95 (2009) 1, 173–179

SURVEY ON IONIC LIQUIDS EFFECT BASED ON METAL ANIONS OVER THE THERMAL STABILITY OF HEAVY OIL

J. A. Murillo-Hernández[1], *S. López-Ramírez*[2*], *J. M. Domínguez*[2], *C. Duran-Valencia*[3], *I. García-Cruz*[2] *and J. A. González-Guevara*[4]

[1]Posgrade Academic Program, IMP, Instituto Mexicano del Petróleo (IMP), Eje Central Lázaro Cárdenas Norte 152 Col. San Bartolo Atepehuacan, México, D.F. 07730, México
[2]Molecular Engineering Research Program, IMP, Instituto Mexicano del Petróleo (IMP), Eje Central Lázaro Cárdenas Norte 152 Col. San Bartolo Atepehuacan, México, D.F. 07730, México
[3]Hydrocarbon Recovery Research Program, IMP, Instituto Mexicano del Petróleo (IMP), Eje Central Lázaro Cárdenas Norte 152 Col. San Bartolo Atepehuacan, México, D.F. 07730, México
[4]GTE-PEP-PEMEX, Av. Marina Nacional 329 Col. Huasteca, Delegación Miguel Hidalo C.P 11311

A survey on the effect of ionic liquids (ILs) over the thermal stability of a heavy Mexican oil was performed. ILs used were based on $[C_nim]^+$ and $[C_npyr]^+$ organic cations with $FeCl_4^-$ metal anion. Mixtures of heavy crude oil (HCO) with ILs show three oxidation zones: low temperature oxidation (LTO), full deposition (FD) and high temperature oxidation (HTO). Thermal stability and mass loss decrease in the LTO zone but increase in the FD and HTO zones for every ILs used. The activation energy of the oxidation is influenced by the ILs in the HTO zone. It decreases when increasing the size of the organic radical substitute in the cation of the ILs while it increases with the presence of hydroxyl groups. The influence of electronic structure and reactivity indexes are rationalized to understand the variations of activation energy obtained of the reaction systems. Among all cations used, cation-3 (IL-3) shows the greater value of HOMO–LUMO gap as well as the lower activation energy.

Keywords: *ab initio calculations, enhanced recovery, heavy crude, ionic liquids, molecular structure, thermal analysis*

Introduction

Oil recovery methods are classified as primary when the oil is associated to the natural drive mechanisms in the reservoir. The secondary processes include water or gas injection to the reservoir while tertiary or enhanced oil recovery employs the injection of foreign materials including an external source of energy (mechanical or thermal). These oil recovery stages is not considered as a chronological sequence [1], for example enhanced recovery methods may be thermal or non thermal; the first ones comprise those whose energy in the reservoir is increased by steam injection for improving the oil transport properties or by chemical reactions for oil upgrading or in-situ flue gas generation [2]. The non-thermal methods are based on the injection of substances with different purpose such as polymers, surfactants, alkaline or gases.

On the other hand, ionic liquids are molten salt under ambient conditions [3] which are formed by cations and anions. Recently, ILs have been applied to organic synthesis [4], catalysis [5], biocatalysis [6], liquid–liquid extraction [7], nanomaterials synthesis [8], polymerization reactions [9], electrochemical [10] and asphaltene precipitation inhibition [11]. The properties of these compounds can be modified by selecting the cation and anion in function of the use envisaged. The most common properties of these compounds are: null or practically null vapor pressure, non-flammablility, catalytic activity, high ionic conductivity, wide range of electrochemical potential, thermal stability, solvent capacity and recyclability [3].

Kök *et al.* investigated the effect of different variables (air [12], pressure [13], °API [14], metallic additives [15], mineral [16, 17], solvent [18]) over the crude oil combustion, by thermal analysis. The effect of air [12] is defined by three distinct reaction regions (LTO, FD and HTO), which were identified in all the crude oils. The variation of total pressure [13] within the range 100–300 psig indicates that the reaction intervals shift from low to higher temperatures when the total pressure increases without any effect on the kinetic parameters. The study of the °API [14] variation revealed that higher activation energy values are obtained in the HTO region when the °API of crude oil decreases. The addition of metallic chloride additives [15] decreases the width of the temperature interval in the three regions and cause the reactions to occur

* Author for correspondence: slopezr@imp.mx

1388–6150/$20.00

Akadémiai Kiadó, Budapest, Hungary
Springer, Dordrecht, The Netherlands

more rapidly with less activation energy. The presence of a limestone matrix [16] proved that the reaction rate in the LTO region is proportional to the specific surface area of the matrix. Likewise, the main properties of the rock (specific surface area, permeability and porosity) are affected during the fuel deposition region. Clays might have a catalytic effect [17] which causes a decrease of the activation energies of combustion reactions of crude oils. Also, the addition of toluene [18] improved the combustion characteristics of the crude oil. Thus, the purpose of the present survey is to expand the before mentioned analysis by including the effect of ILs over the thermal stability of heavy oil under combustion conditions.

The molecular structure of some ionic liquids with models in the gas phase have been studied using different levels of theory, semi-empirical, ab initio and by means of the density functional theory (DFT) [19–22]. Some studies have shown the use of the ionic liquids for promoting some catalytic reactions [23–25]. For example, Suarez *et al.* [26] used new ionic liquids as catalyst for hydrogenation reactions using rhodium complexes, whereas Earle *et al.* [27] studied the influence of the ionic liquids over the yield and selectivity of the reaction between aromatic compounds and nitric acid. The ionic liquids having metal halide anions in their structure show Lewis acidity, especially those based on $FeCl_4^-$ anion. Thus, the influence of the ILs molecular structure of the activation energy and thermal stability of heavy oil were investigated by ab initio calculations. This analysis included a systematic study of the electronic structure and various reactivity indexes, for instance, the HOMO–LUMO gap, the electronegativity and the hardness of the ionic liquids cation.

Experimental

Heavy oil from 'Angostura' oil field located in south México was used for this survey; its physical and chemical properties are summarized in Table 1. Table 2 shows the series of ionic liquids that were synthesized for the present survey [28, 29]. The ILs were synthesized from two principal families of $[C_nim]^+$ and $[C_npyr]^+$ cations, respectively. To assure higher integration and homogeneity in the oil, ILs were dissolved firstly in acetonitrile and this mixture was added to oil with a final concentration of 0.12 mass% of ILs.

The thermal analysis was carried out in a Perkin Elmer TGA-7 Thermogravimetric Analyzer. A flow of 20 mL min^{-1} of high purity extra dry air was used as a dragging gas. Samples of approximately 10 mg were heated from room temperature up to 1000°C at a heating rate of 5°C min^{-1}.

Table 1 Physical and chemical properties from Angostura oil

Physical properties	
Molecular mass/u	459
°API	12.2
Viscosity/cP, at 25°C	22500
Chemical composition	
Sulphur/mass%	5.22
Carbon/mass%	83.85
Hydrogen/mass%	10.13
Nitrogen/mass%	0.65
Oxygen/mass%	0.15
SARA analysis	
Saturates/mass%	21.04
Aromatics/mass%	33.41
Resins/mass%	18.87
Asphaltene/mass%	26.04

Kinetic analysis

The combustion reaction of oil is a complex phenomenon, which can be simplified using an excess of air. Kök *et al.* reported a simple kinetic model relating the mass change rate with the Arrhenius equation, to calculate the activation energy, as follows [16]:

$$\log\left[\frac{\left(\frac{dW}{dt}\right)}{W}\right]=\log A-\frac{E_a}{2.303R}\frac{1}{T} \qquad (1)$$

In this expression the activation energy of the combustion reaction is determined from the slope of the straight line.

Computational details

The minimun-energy geometries of the ILs used in the present work, i.e. $[C_ndmim]^+$, $[C_npyr]^+$ cations, and $FeCl_4^-$ anion, were determined by ab initio geometry optimizations at the B3LYP/6-31(d,p) level [30–32] using de Gaussian 98 package program [33]. A vibrational analysis was performed to ensure the absence of negative frequencies and the existence of true minima was verified. Both, electronic structure and properties were analyzed, i.e. HOMO–LUMO energy gap (Δ_{H-L}), the electronegativity (χ), and the absolute hardness (η), according to the following expressions:

$$\chi=\frac{(I+A)}{2} \qquad (2)$$

Table 2 Ionic liquids used in this survey

IL	Cation	Anion	Name
IL–1	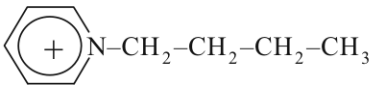	$FeCl_4^-$	[Bpyr][$FeCl_4$]
IL–2	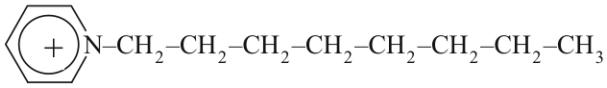	$FeCl_4^-$	[Opyr][$FeCl_4$]
IL–3	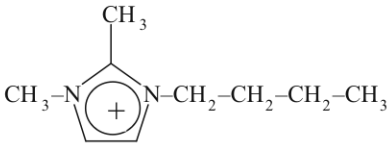	$FeCl_4^-$	[Bdmim][$FeCl_4$]
IL–4	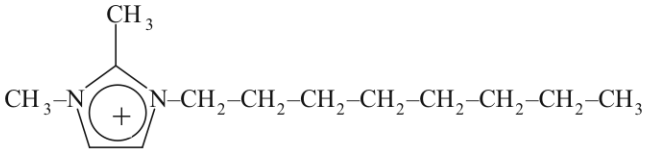	$FeCl_4^-$	[Odmim][$FeCl_4$]
IL–5	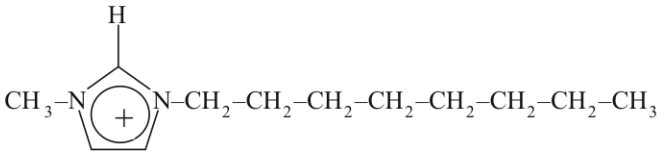	$FeCl_4^-$	[Omim][$FeCl_4$]
IL–6	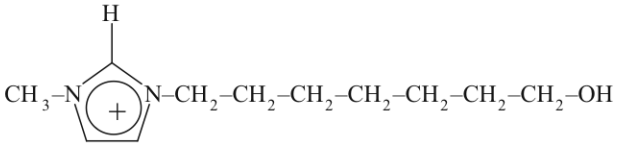	$FeCl_4^-$	[Hhmim][$FeCl_4$]

$$\eta = \frac{(I - A)}{2} \quad (3)$$

where I and A are the ionization potential and electronic affinities of the chemical system, atom, ion, molecule or radical [34]. Within the validity of Koopmans' theorem [35], the frontier orbital energies are given by:

$$-\varepsilon_{HOMO} = I \quad (4)$$

$$-\varepsilon_{LUMO} = A \quad (5)$$

Results and discussion

The oil combustion experiments led to verification of three reaction zones from the TG/DTG curves (Figs 1 and 2). The first zone ranges from room temperature up to 380°C and it is recognized as a low temperature oxidation (LTO). The second zone ranging from 380 up to 500°C which is identified as fuel deposition zone (FD), while the last zone is known as a high temperature oxidation region (HTO) which ranges from 400 up to 700°C [12, 14].

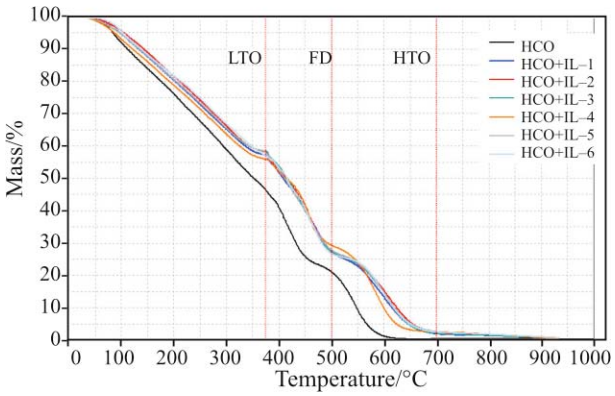

Fig. 1 TG curve of crude oil and mixtures with ILs

Figure 1 shows that all mixtures of heavy crude oil with ILs (HCO+ILs) present a decreasing profile with oxidation temperature with respect to the origi-

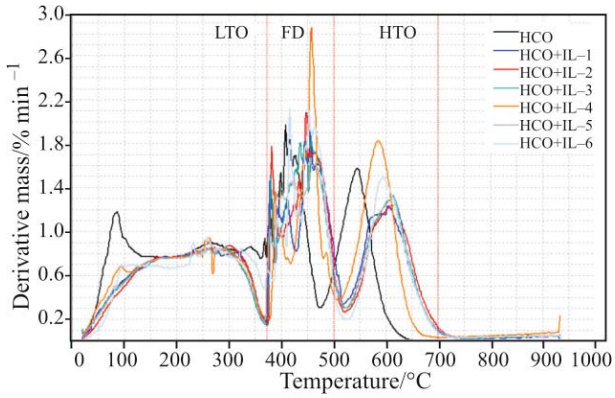

Fig. 2 DTG curve from crude oil and mixtures with ILs

Table 3 Reaction interval from the combustion reaction of oil samples

Sample	LTO/°C	FD/°C	HTO/°C
HCO	20–389	389–474	474–656
HCO+IL-1	20–372	372–518	518–761
HCO+IL-2	20–375	375–521	521–746
HCO+IL-3	20–374	374–523	523–755
HCO+IL-4	20–377	377–508	508–700
HCO+IL-5	20–368	368–521	521–745
HCO+IL-6	20–366	366–524	524–732

nal crude, which provokes modifications in the reaction interval. Table 3 shows the values from reaction intervals for each reaction zone for all the mixture series; one observes that in the LTO zone all the mixtures of HCO with ILs show a decrease of the reaction interval value to average of 4.5%. In the reaction interval FD and HTO zones the effect of ILs over the HCO was the opposite, as shown in the reaction intervals that increased for an average of 73.1 and 21.3%, respectively.

Also, there is an influence of ILs on the mass loss during combustion reaction in each oxidation zone. In Table 4 the total mass loss is reported for each sample together with a description for each zone.

Table 4 Mass loss for crude oil samples

Sample	LTO/%	FD/%	HTO/%
HCO	56.26	20.40	23.34
HCO+IL-1	42.74	31.69	25.57
HCO+IL-2	41.89	32.32	25.80
HCO+IL-3	41.61	32.83	25.56
HCO+IL-4	44.28	27.05	28.68
HCO+IL-5	41.53	32.30	26.17
HCO+IL-6	42.18	32.39	25.43

In the LTO region the mass loss decreased about 24.7%, but in the FD and high oxidation HTO zones the effect of ILs seems different, because the mass loss increases by about 54.0 and 12.3%, respectively.

The DTG curves from HCO and its mixtures with ILs (Fig. 2) show significant changes in the maximum rate of decomposition together with its corresponding temperature, and final combustion temperature. Table 5 shows the values of maximum rate, the temperature of maximum rate for each zone and the final combustion temperature for all the samples.

From the results reported in Table 5, one observes that within the LTO zone all the ILs caused a decrease of decomposition rate for about 24.8%, while the maximum temperature of decomposition increased to average 188.4°C. In the FD zone the IL-1, IL-3 and IL-5 provoke a decrease of about 7.93% of the decomposition rate; however, IL-2, IL-4 and IL-6 provoked an increase of about 19.5% in the decomposition rate.

All the ILs applied in this work provoke an increase of about 40.4°C in the maximum decomposition temperature. Regarding the HTO zone only the IL-4 caused an increase of 15.6% in the decomposition rate, while the remaining ILs decreased the decomposition rate for about 16.5%. All the ILs caused an increase of about 59.0°C in the maximum decomposition temperature which implies a higher stability of the oil. Also, the final combustion temperature increased in all cases for an average of 84°C.

Table 5 Peak from each region and combustion temperature of the mixture of oil and ILs

Sample	Peak LTO		Peak FD		Peak HTO		Total burnout/°C
	rate/ % min^{-1}	°C	rate/ % min^{-1}	°C	rate/ % min^{-1}	°C	
HCO	1.18	86	1.97	409	1.58	546	656
HCO+IL-1	0.85	265	1.93	457	1.23	604	761
HCO+IL-2	0.87	302	2.09	448	1.24	618	746
HCO+IL-3	0.86	293	1.87	458	1.33	615	755
HCO+IL-4	0.94	264	2.86	458	1.83	585	700
HCO+IL-5	0.85	261	1.65	457	1.30	611	745
HCO+IL-6	0.95	259	2.12	416	1.49	595	732

Thus, the use of ILs follow a decreasing trend in the percentage of mass loss in the LTO zone, making it less resistant to temperature, but the introduction of ILs increase the mass loss in the decomposing process for the FD and HTO zones, thus causing a higher resistance to temperature. Due to the fact that ILs are composed entirely of cations and anions, the interaction of these compounds with HCO should be higher with its polar components like asphaltenes. The asphaltenes are compounds with poly-aromatics rings and heteroatoms that contain electron donor-acceptor pairs as well as a high molecular mass and a high boiling point. Therefore, the kinetic in HTO zone is more important because asphaltenes are located in this region. Recently, the possible interaction of asphaltenes with the heteroatoms compounds has been studied both at a theoretical and experimental level [36–38].

Figure 3 shows the thermal stability differences among the HCO and its mixtures with ILs (HCO+LIs) in the HTO zone. This behavior is analyzed by means of the activation energy obtained from the kinetic analysis. The activation energy is obtained from the plot $\log(dW/dt)/W$ *vs.* $1/T$ using the TG/DTG curves. Figure 4 shows Arrhenius curves obtained from all

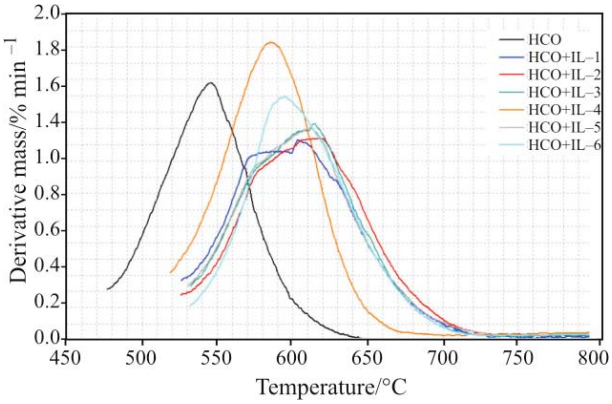

Fig. 3 DTG curve from crude oil and ILs mixtures in the HTO zone

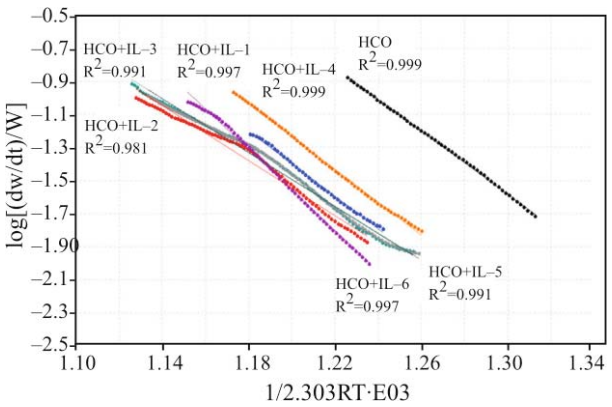

Fig. 4 Arrhenius curve from crude oil and the ILs mixtures in the HTO zone

Table 6 The activation energies in the HTO zone

Sample	E_a/kJ mol^{-1}	R^2*
HCO	182.54	0.999
HCO+IL-1	189.18	0.997
HCO+IL-2	158.74	0.981
HCO+IL-3	156.99	0.991
HCO+IL-4	189.99	0.999
HCO+IL-5	156.01	0.991
HCO+IL-6	235.64	0.997

*Correlation factor

the samples analyzed. The value of activation energy for each sample is calculated from the slope (m=($-E_a$)/2.303R) obtained in each fitted curve.

Table 6 shows activation energy values and the correlation coefficient for each sample. From these data the correlation coefficients show an average of r=0.994, which indicates that the correctness of the assumption of a reaction order equals to one for the combustion reaction of the HTO zone. Regarding the activation energy values, it is observed that IL-1, IL-4 and IL-6 provoke an increase of the energy to decompose molecules found in this reaction zone, while IL-2, IL-3 and IL-5 decreased the amount of energy needed to crack molecules within the HTO zone.

On the other hand, the electronic structure calculation can give us a possible explanation on the variation of the activation energy, although the approach is in gas phase. At present, this research group is working on detailed studies of electronic structure and molecular dynamics of HCO+ILs systems.

Table 7 shows the different reactivity indexes, such as the HOMO–LUMO gap, and the electronegativity of cation and anion of the ionic liquids. The HOMO–LUMO gap shows a small change for the different cations, 4.03 to 6.59 eV. The HOMO–LUMO gap for the cation-3 (IL-3) is 6.59 eV. Cation-3 shows the greater HOMO-LUMO gap value compared to the other $[C_n im]^+$ cations, and this can be the reason which the IL-3 shows the lowest activation energy. In this case, the IL-3 is formed by $[Bdmim]^+$ cation and $FeCl_4^-$ anion. For the cation-4 and the cation-5, the values HOMO–LUMO gap are similar, the average values between both cations is 5.8 eV. These ILs are formed by $[Odmim]^+$ and $[Omim]^+$ cations, respectively.

The HOMO–LUMO gap for the cation-6 displays a value of 4.09 eV and this probability may be due to the presence of a hydroxyl group in this structure. Whereas, the HOMO–LUMO gap values for cation-1 and cation-2 are 5.77 and 4.03 eV respectively, showing only a difference of 1.7 eV among them. These ILs are derived from $[C_n pyr]^+$ cation. While HOMO energies show a small variation, the LUMO

Table 7 Theoretical calculation of the reactivity indexes for cations and anions from ILs

Molecules	HOMO	LUMO	Δ_{H-L}/eV	*I*	*A*	χ	η
Cation							
Cation-1	–0.449	–0.237	5.77	0.449	0.237	0.343	0.106
Cation-2	–0.384	–0.236	4.03	0.384	0.236	0.309	0.074
Cation-3	–0.410	–0.168	6.59	0.410	0.168	0.289	0.121
Cation-4	–0.386	–0.166	5.97	0.386	0.166	0.276	0.109
Cation-5	–0.386	–0.176	5.73	0.386	0.176	0.281	0.105
Cation-6	–0.326	–0.176	4.09	0.326	0.176	0.251	0.075
Anion							
$FeCl_4^-$	–0.149	0.009	0.158	0.149	–0.009	0.070	0.079

energies show the opposite. The larger variation of LUMO energies may be a result of the increase of the electron affinity of the cation. In this context, cation-3 presents a greater value of HOMO, which means a higher electronegativity and hardness with respect to the other cations. This behavior probably will favor acid catalysis, through nucleophilic attack in the reaction between the ILs and the asphaltenes and this is the reason for which there is a smaller activation energy. The other cations studied present a minor value of HOMO, a lower electronegativity and less hardness which may favor an electrophilic attack in these reactions.

The electronegativity and hardness of cations values studied in this research show a very similar tendency to the HOMO–LUMO gap values. Cation-3 shows the greater value of electronegativity and hardness with regards to the other ILs derived from the $[C_nim]^+$ cations, whereas the values of electronegativity for cation-1 and cation-2 are 0.343 and 0.309, respectively. The value of electronegativity of cation-2 is similar to cation-3 and cation-5, which show low activation energy with regard to the other ILs. Therefore, its molecular structure is different; IL-3 and IL-5 are derivatives of $[C_nim]^+$ cations, while IL-2 is derivative of $[C_npyr]^+$ cations. The variation of the activation energies may be related with the molecular structure and the different reactivity indexes of $[C_nim]^+$ and $[C_npyr]^+$ cations used and the asphaltene found in the oil heavy fraction.

The molecular structures of IL-1 and IL-2 are similar but their molecular size is different depending of the substituted radical in the $[C_npyr]^+$ cation. The activation energy of the HCO is increased by effect of IL-1, but its value is decreased by effect of IL-2; this might be related to the fact that IL-2 counts on a higher size substitute, this impeding the clustering of asphaltene molecules and making oil thermal decomposition easier. Comparing the activation energy between the systems HCO+IL-3 and HCO+IL-5, both present the similar activation energies. The difference between these is the organic tail size, while IL-3 has a small tail IL-5 shows a larger one. The similarity in the activation energy probability is due to HOMO–LUMO gap, previously discussed.

Finally, the molecular structures of IL-5 and IL-6 are similar; however IL-6 contains a hydroxyl group at the end of the substituted radical in the $[C_nim]^+$ cation. This hydroxyl group produces a stronger interaction with asphaltene, probably through the formation of hydrogen bonds between the molecules which is consistent, due to the fact that the activation energy needed to decompose the system HCO+IL-6 is higher than the system HCO+IL-5.

Conclusions

In summary, the present research analyzed the thermal stability of crude heavy oil by means of different experimental techniques and a correlation was sought with the electronic structure and various reactivity indexes studies.

From results obtained experimentally through this survey, the following can be stated: both, pure HCO and its mixtures with ILs (HCO+ILs), showed three oxidation zones labeled LTO, FD and HTO, just as it has been published in other investigations [12–14, 16]. By means of the termogravimetric analyses, it was observed that all ILs surveyed affect oil thermal stability by decreasing it in the LTO zone and increasing it in FD and HTO zones, and modifying the amount of mass loss in the different combustion zones. In the LTO zone the amount of mass loss decreased in all cases; however the amount of mass loss increased in the FD and HTO zones.

Based on the values of the correlation coefficients obtained, it is confirmed that the kinetic model used to calculate the activation energy for the combustion reaction in the HTO zone is acceptable, just as it has been published in other studies [12–14, 16].

On the other hand, the variation of the activation energies related to the different reactivity indexes from $[C_n im]^+$ and $[C_n pyr]^+$ cations used and the asphaltene found in the oil heavy fraction can be explained through the studies of the electronic structure. The HOMO–LUMO gap for cation-3 (IL-3) is 6.59 eV. This cation shows the greatest HOMO–LUMO gap value in comparison to the other $[C_n im]^+$ cations, and probably this is the reason that IL-3 shows low activation energy, compare to the other ILs.

When increasing the size of the substituted radical in similar cations in ILs, a decrease in activation energy is produced in the mixtures due to the steric hindrance effect from molecules, except to cation-3, already discussed. The presence of a hydroxyl group in the radical substituted of a cation, originates an activation energy increase in the system due to the formation of hydrogen bonding among the molecules.

Acknowledgements

Authors thank the Mexican Petroleum Institute and PEMEX for the economic support granted to Project Research F.24224. J. A. Murillo-Hernández thanks CONACYT and the IMP for the economic support granted during his Ph.D. studies.

References

1 D. W. Green and G. P. Willhite, Enhance Oil Recovery, SPE Texbook Series, Texas 1998, p. 1.
2 A. Farouq and S. Thomas, J. Can. Pet. Technol., 39 (2000) 2.
3 P. Wasserscheid and W. Keim, Angew. Chem. Int. Edit., 39 (2000) 3773.
4 T. Welton, Chem. Rev., 99 (1999) 2071.
5 D. Zhao, M. Wu, Y. Kou and E. Min, Catal. Today, 74 (2002) 157.
6 R. A. Sheldon, L. Maderia, M. Sorgedrager and K. R. Seddon, Green Chem., 4 (2002) 147.
7 R. P. Swatloski, A. E. Visser, W. M. Reichert, G. A. Broker and L. M. Facina, Green Chem., 4 (2002) 81.
8 E. J. Rohling, R. March, N. C. Wells, M. Siddall and N. R. Edwards, Nature, 430 (2004) 1012.
9 H. R. Kricheldorf and G. Schwarz, High Perform. Polym., 16 (2004) 543.
10 C. Yang, Q. Sun, J. Qiao and Y. J. Li, J. Phys. Chem. B, 107 (2003) 12981.
11 Y. F. Hu and T. M. Guo, Langmuir, 21 (2005) 8168.
12 M. V. Kök, Thermochim. Acta, 214 (1993) 315.
13 M. V. Kök, R. Hughes and D. Price, Thermochim. Acta, 287 (1996) 91.
14 M. V. Kök and C. Keskin, Thermochim. Acta, 369 (2001) 143.
15 M. V. Kök and A. G. Iscan, J. Therm. Anal. Cal., 64 (2001) 1311.
16 M. V. Kök, G. Pokol, C. Keskin, J. Madarász and S. Bagci, J. Therm. Anal. Cal., 75 (2004) 781.
17 M. V. Kök, J. Therm. Anal. Cal., 84 (2006) 361.
18 A. G. Iscan, M. V. Kök and A. S. Bagci, J. Therm. Anal. Cal., 88 (2007) 653.
19 J. H. Antony, D. Mertens, T. Breitenstein, A. Dölle, P. Wasserscheid and W. R. Carper, Pure Appl. Chem., 76 (2004) 255.
20 E. R. Talaty, S. Raja, V. J. Storhaug, A. Dölle and W. R. Carper, J. Phys. Chem. B, 108 (2004) 13177.
21 J. L. Anthony, E. J. Maginn and J. F. Bennecke, J. Phys. Chem. B, 106 (2002) 7315.
22 Z. Meng, A. Dölle and W. R. Carper, Theochem. J. Mol. Struct., 585 (2002) 119.
23 R. Sheldon, Chem. Commun., 23 (2001) 2399.
24 J. S. Wilkes, J. Mol. Catal. A-Chem., 214 (2004) 11.
25 H. Xing, T. Wang, Z. Zhou and Y. Dai, J. Mol. Catal. A-Chem., 264 (2007) 53.
26 P. A. Z. Suares, J. E. Dullius, S. Einloft, R. F. De Souza and J. Dupont, Polyhedron, 15 (1996) 1217.
27 M. J. Earle, S. P. Katdare and K. R. Seddon, Org. Lett., 6 (2004) 707.
28 Y. J. Kim and R. S. Varma, Tetrahedron Lett., 46 (2005) 1467.
29 Y. J. Kim and R. S. Varma, J. Org. Chem., 70 (2005) 7882.
30 A. D. Becke, J. Chem. Phys., 98 (1993) 5648.
31 C. Lee, W. Yang and R. G. Parr, Phys. Rev. A, 38 (1988) 3098.
32 W. J. Hehre, R. Ditchfield and J. A. Pople, J. Chem. Phys., 56 (1972) 2257.
33 M. J. Frisch, G. W. Trucks, H. B. Schlegel, G. E. Scuseria, M. A. Robb, J. R. Cheeseman, V. G. Zakrzewski, J. A. Montgomery Jr., R. E. Stratmann, J. C. Burant, S. Dapprich, J. M. Millam, A. D. Daniels, K. N. Kudin, M. C. Strain, O. Farkas, J. Tomasi, V. Barone, M. Cossi, R. Cammi, B. Mennucci, C. Pomelli, C. Adamo, S. Clifford, J. Ochterski, G. A. Petersson, P. Y. Ayala, Q. Cui, K. Morokuma, D. K. Malick, A. D. Rabuck, K. Raghavachari, J. B. Foresman, J. Cioslowski, J. V. Ortiz, A. G. Baboul, B. B. Stefanov, G. Liu, A. Liashenko, P. Piskorz, I. Komaromi, R. Gomperts, R. L. Martin, D. J. Fox, T. Keith, M. A. Al-Laham, C. Y. Peng, A. Nanayakkara, C. Gonzalez, M. Challacombe, P. M. W. Gill, B. Johnson, W. Chen, M. W. Wong, J. L. Andres, C. Gonzalez, M. Head-Gordon, E. S. Replogle and J. A. Pople, Gaussian 98, Revision A.7, Gaussian Inc., Pittsburgh PA 1998.
34 R. G. Pearson, Inorg. Chem., 27 (1986) 734.
35 T. Koopmans, Physica, 1 (1934) 104.
36 I. García-Cruz, J. M. Martínez-Magadán, P. Guadarrama, R. Salcedo and F. Illas, J. Phys. Chem. A, 107 (2003) 1597.
37 H. Groenzin and O. Mullins, J. Phys. Chem. A, 103 (1999) 11237.
38 H. Groenzin and O. Mullins, Energy Fuels, 14 (2000) 677.

Received: December 10, 2007
Accepted: May 6, 2008
OnlineFirst: September 20, 2008

DOI: 10.1007/s10973-007-8919-5